WPHCD-PR(18) 21275

P Kalaria et al.

Multi-physics Modelling of Insert Cooling System for an 170 GHz, 2 MW Long-pulse Coaxial-cavity Gyrotron

Preprint of Paper to be submitted for publication in
IEEE Transactions on Electron Devices

This work has been carried out within the framework of the EUROfusion Consortium and has received funding from the Euratom research and training programme 2014-2018 under grant agreement No 633053. The views and opinions expressed herein do not necessarily reflect those of the European Commission.

This document is intended for publication in the open literature. It is made available on the clear understanding that it may not be further circulated and extracts or references may not be published prior to publication of the original when applicable, or without the consent of the Publications Officer, EUROfusion Programme Management Unit, Culham Science Centre, Abingdon, Oxon, OX14 3DB, UK or e-mail Publications.Officer@euro-fusion.org

Enquiries about Copyright and reproduction should be addressed to the Publications Officer, EUROfusion Programme Management Unit, Culham Science Centre, Abingdon, Oxon, OX14 3DB, UK or e-mail Publications.Officer@euro-fusion.org

The contents of this preprint and all other EUROfusion Preprints, Reports and Conference Papers are available to view online free at http://www.euro-fusionscipub.org. This site has full search facilities and e-mail alert options. In the JET specific papers the diagrams contained within the PDFs on this site are hyperlinked

Multi-physics Modelling of Insert Cooling System for an 170 GHz, 2 MW Long-pulse Coaxial-cavity Gyrotron

P. C. Kalaria[1], M. George[1], S. Illy[1], K. A. Avramidis[1], G. Gantenbein[1], S. Ruess[1], M. Thumm[1,2] and J. Jelonnek[1,2]
[1]Institute for Pulsed Power and Microwave Technology (IHM),
[2]Institute of Radio Frequency Engineering and Electronics (IHE),
Karlsruhe Institute of Technology (KIT), Karlsruhe, Germany.

E-mail: parth.kalaria@kit.edu

Abstract. High-power, high-frequency gyrotrons are the only promising sources for the Electron Cyclotron Resonance Heating and Current Drive (ECRH&CD) in present thermonuclear fusion plasma experiments and in future power plants. Compared to the hollow-cavity gyrotron design, the coaxial cavity gyrotron design facilitates improved mode competition control, which eventually increases the output power per tube. At KIT-IHM, the successful operation of a 170 GHz gyrotron has been demonstrated in the short-pulse regime and the ongoing research activities are aiming to upgrade the existing coaxial cavity gyrotron from short-pulse (1-10 ms) to long-pulse (~ 1 s) operation. In this work, with the help of multi-physics simulations, the performance of the insert cooling system is verified for the continuous wave (CW) operation and the operating limits of the insert cooling systems are determined. The perfectly aligned coaxial Glidcop insert will be able to withstand operating conditions leading to a maximal heat flux of about 0.39 kW/cm^2. The influence of insert misalignment on insert loading is also studied systematically in this work.

Keywords. Nuclear fusion, Electron Cyclotron Resonance Heating and Current Drive (ECRH&CD), Gyrotron, Coaxial cavity, Insert loading analysis, Insert misalignment, Thermal-hydraulic simulations, Thermo-mechanical simulations

1. Introduction

A gyrotron is a vacuum tube producing high-power (ranging from tens of kW to several MW) RF wave in the sub-millimetre/millimetre wave frequency range [1-3]. The prime applications of high power (~ 1-2 MW), high frequency (70 GHz to 300 GHz) gyrotrons include electron cyclotron resonance heating (ECRH), non-inductive Current Drive (CD), plasma stability control and plasma diagnostics in thermo-nuclear fusion experiments. As an example, for the Wendelstein 7-X (W7-X) stellarator in Greifswald (Germany), in total ten 140 GHz, 1 MW CW (1800 s) hollow-cavity gyrotrons are completely installed and are being operated successfully to fulfil the total ECRH requirement [4]. For the ITER tokamak in Cadarache (France), 24 Continuous Wave (CW) (~ 3600 s) gyrotrons with an operating frequency of 170 GHz are planned for a total power requirement of 20 MW [5-8]. Following the successful operation of ITER, the DEMOnstration power plant (DEMO) is proposed [9]. It will be the first fusion power plant, which will notably intend to generate net electric power. According to the current baseline, the operating frequencies for heating and current drive of DEMO are expected to be 170/204 GHz [10-12]. At KIT-IHM, conceptual design studies on the DEMO gyrotrons and the development of the related technologies are ongoing as a part of the EUROfusion work-package [13-19].

For ITER, a 1 MW, 170 GHz hollow-cavity gyrotron and a 2 MW, 170 GHz coaxial cavity gyrotron have been developed by the European GYrotron Consortium (EGYC) in cooperation with the industrial partner Thales Electron Devices (TED) [20-21]. At KIT, the operation of the industrial prototype of the hollow-cavity ITER gyrotron was successfully verified with the pulse lengths of up to 180 s, which is the

maximum possible pulse length at the KIT test facility [22]. To further increase of the gyrotron pulse duration, further experiments are being performed at Swiss Plasma Center (SPC), Lausanne. The record output power of 2.2 MW has been reported for the EU 170 GHz coaxial-cavity gyrotron for short-pulse operation in the range of a few milliseconds [23]. The existing components of the short-pulse coaxial-cavity gyrotron are being upgraded for the long-pulse operation [24]. Along with the European Union (EU), the development of 170 GHz ITER gyrotrons is ongoing at the Institute of Applied Physics (IAP), Russia, with the industrial partner GYCOM and at the National Institute for Quantum and Radiological Science and Technology (QST), Japan, with the industrial partner TOSHIBA [25-27].

A simple schematic of the coaxial-cavity gyrotron is presented in Figure 1**.** In the case of the coaxial-cavity design, an additional longitudinally corrugated insert is placed at the cavity center. The insert is supported in the Magnetron Injection Gun (MIG) and then extended through the beam-tunnel and cavity up to the quasi-optical launcher through the beam-tunnel and cavity (See Figure 1). Compared to the hollow-cavity design, the corrugated-insert significantly controls the mode competition and reduces the effects of space-charge during the start-up, which allows high-power gyrotron operation in a very high-order operating mode. During the gyrotron operation, the cavity surface and the coaxial insert are heated by the generated RF wave. The increase in temperature results in deformations of the cavity wall and the insert, which further modify the frequency of the generated RF wave and the total heat flux. For the selected gyrotron design (170 GHz coaxial-cavity gyrotron), according to first calculations, the heat flux can reach up to 1.64 kW/cm^2 at the cavity wall and 0.11 kW/cm^2 on the insert. To mitigate the adverse effects of the increased temperature and resulting material deformations, the cavity surface and the insert are water-cooled. The performance of the cavity cooling system is studied systematically in [28-31].

In this work, the performance of the insert cooling system is numerically verified for the continuous wave (CW) operation of a 170 GHz, 2 MW gyrotron. The schematic of the insert cooling system is presented in Figure 2. The water flows up to the top of the insert in a central inlet pipe and then flows down between the pipe's outer wall and the inner inlet wall. With the nominal operating conditions, it had to be checked that the insert would be able to withstand CW operation without significant deformation. The selected iterative simulation approach for the insert cooling system analysis is discussed in section 2. In section 3, the effectiveness of the existing insert cooling system of a 170 GHz short-pulse prototype is checked for the CW gyrotron operation. The operational limits of the insert cooling system are also investigated with respect to the maximum allowable wall-loading and insert radius. The influence of the axial insert misalignment on a cooling efficiency is systematically studied in section 4.

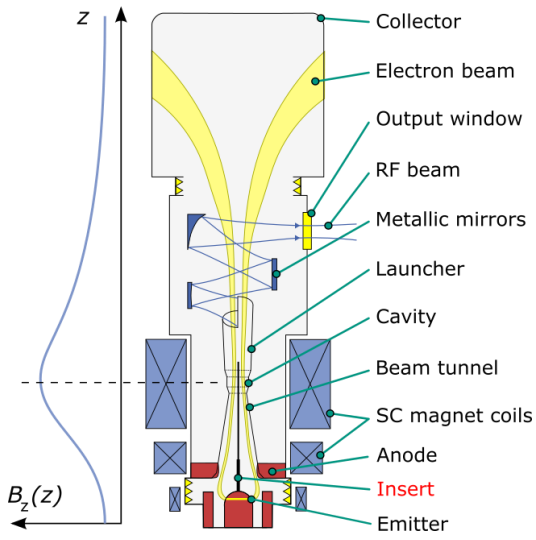

Figure 1: Schematic of a coaxial cavity gyrotron with axial magnetic field profile.

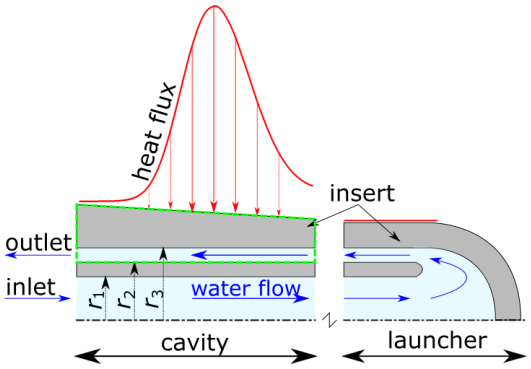

Figure 2: Simple sketch of the existing insert cooling system with the heat flux profile. The values of r_1, r_2 and r_3 are 3 mm, 4 mm and 5 mm, respectively. The selected sector for the multi-physics simulations is highlighted with the green dashed line.

2. Simulation set-up for multi-physics analysis

2.1 Overview of the simulation set-up

The overview of the applied simulation approach is given in Figure 3. For this purpose, an iterative study is carried out for each case in the following way. First, with help of the electromagnetic (EM) simulation (also named as beam-wave interaction simulation), the heat flux corresponding to the original geometry is calculated at room temperature. The calculated heat flux is imposed on the insert wall to obtain the temperature field profile in the thermal-hydraulic (TH) simulation. In the next step, the deformations of the structure are calculated in the thermo-mechanical (TM) simulation using the new temperature profile. The deformed geometry and new temperature profile are then used for the calculation of the new heat flux in EM simulation. These steps are iterated until a convergence of the calculated heat fluxes is obtained or unacceptable results (boiling of the cooling water or plastic deformations of the insert) are encountered.

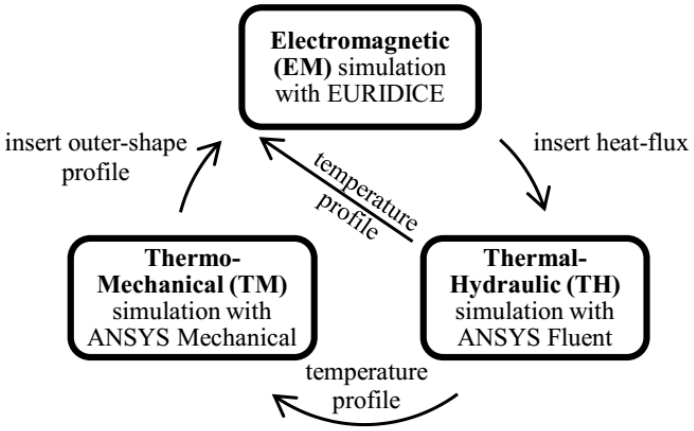

Figure 3: Overview of the selected iterative simulation approach.

The EM simulations are performed with the code-package EURIDICE [32], while the software suite ANSYS (version 18.0) is used for the TH and TM simulations. Two code-packages are mainly used, namely ANSYS Fluent for the TH and ANSYS Mechanical for the TM simulations. The CAD models of the insert and cavity of a 170 GHz gyrotron are presented in Figure 4. The total length of the insert is 1403 mm and it is mounted at the electron gun region. The cavity is placed at the axial distance of 1100 mm and the total length of the cavity is 152 mm. The inner radius of the water inlet is 3 mm and the thickness of the inlet pipe is 1 mm (refer Figure 2). The zone where water flows down, between the outer wall of the inlet pipe and the insert inner-wall is also 1 mm thick. As the value of the insert heat flux is negligible outside the cavity region, it is not considered in the simulations to manage computational resources. The selected radial profiles of the cavity inner-wall and the insert outer-wall are plotted in Figure 5, in which, the values minimum and maximum insert radius are 7.197 mm and 8.384 mm, respectively, while the values of minimum and maximum cavity radius are 17 mm and 32.5 mm.

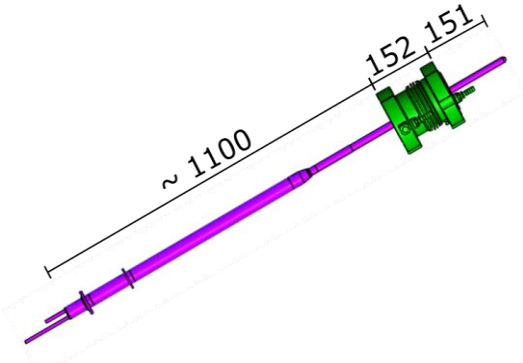

Figure 4: CAD models of the insert and cavity of a 170 GHz longer-pulse gyrotron. All the dimensions are in millimeter.

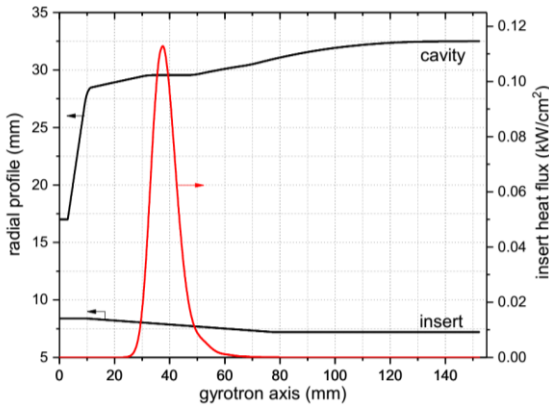

Figure 5: Radial profiles of the selected cavity and insert section. The insert heat flux profile at nominal operating condition is also shown along the gyrotron axis.

2.2 Beam-wave interaction simulation

For the particular cavity/insert profiles and the selected gyrotron operating parameters, the beam-wave interaction simulations are performed to estimate the gyrotron performance and calculate the heat load profile of the insert. In this case, the heat load is the average disperse power due to ohmic loading, which can be calculated using [33],

$$\rho = \frac{1}{2\sigma\delta} |H_{\mathrm{t}}|^2 \tag{1}$$

Here, ρ is the ohmic wall loading, H_{t} is the tangential magnetic component of the RF field, σ is the conductivity of the material and δ is the skin depth. In the short-pulse prototype, a copper insert was used, which will be replaced with an insert made of GlidCop Al-15 for a longer-pulse gyrotron. GlidCop Al-15 is a copper alloy, which is extensively used at high power operation over copper due to its advanced mechanical properties [34]. A consideration of the operating frequency and temperature-dependent skin depth and conductivity of the GlidCop AI-15 material are included in the EM simulations. Additionally, the influence of the insert corrugations is considered for the interaction calculations. For the first iteration, the uniform temperature of 27 °C is selected for the cavity and insert with the standard non-deformed geometry (see Figure 5). The updated temperature profiles from the TH simulations and deformed insert profiles from the TM simulations are considered in the successive iterations. The realistic magnetic field profile with maximum field strength of 6.89 T is used for the iterations with the beam energy of 90 keV, beam current of 75 A and pitch factor of 1.3. The insert-loading profile for the first iteration is shown in Figure 5**.**

2.3 Thermal-hydraulic simulation

Considering the symmetry of the aligned insert and the heat-flux, it is possible to manage computational effort using the rotational periodic boundary condition. To validate this approach, as an initial step, a 10° and 20° slices of the insert were selected as a simulation domain with the rotational periodic boundary conditions. A 90° slice was also simulated by selecting two planes of symmetry. The results of the discussed cases were almost the same within a 1°C range of the extremal temperatures in the solid and in the water. Finally, the 10°-degree slice of the insert was selected for the further analysis (See Figure 6).

The SST (Shear-Stress Transport) k-ω turbulence model is adopted in our analysis. The maximum mesh cell length in the axial direction is 0.1 mm, which matches the accuracy of the data provided by EURIDICE. The selection of mesh parameters is discussed in detail in the Appendix.

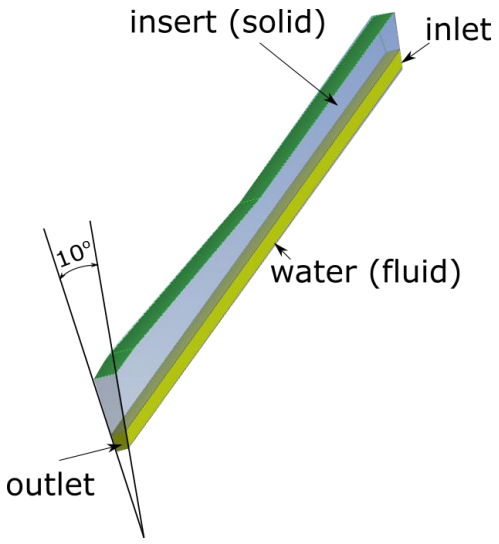

Figure 6: 10°-degree slice of the insert selected for the TH simulations in ANSYS fluent.

The insert heat flux provided by the EM simulation is imposed to the outer wall of the insert. At the inlet of the fluid domain, a flow speed of 5.9 m/s is imposed, which for the adopted dimensions corresponds to a 10 L/min flow rate. This is the maximum flow rate (with a reasonable security margin) that supports the operation of the insert without significant vibration.

2.4 Thermo-mechanical simulation

The insert geometry is imported in ANSYS Mechanical for TM simulation. It is meshed using a uniform sizing function with a maximum element size of 0.1 mm in the axial direction. The temperature field imported from TH is considered as the load. As the heat-flux on the non-represented lower part of the coaxial insert is negligible, this part is neither deformed nor displaced. Therefore, a fixed-support condition is imposed on the lower face of the selected insert domain. The cyclicity condition (which is equivalent to the rotational periodicity condition used in TH simulation) imposed to the lower and upper boundaries of the represented angular sector guarantees that the model corresponds to the real problem. Without this condition, the software considers the represented domain as a whole solid body, which is then free to move with no other constraint than the fixed base, which leads the body to bend in the direction opposite to the temperature gradient. GlidCope AI-15 material is considered with the density of 8830 kg/m^3 (value at 100 °C), the coefficient of thermal expansion of 1.7 × 10^{-5} /°C, Young's modulus of 117 GPa and a Poisson's ratio of 0.33.

3. Insert cooling system: perfectly aligned case

As a first step, the existing insert cooling system of a 170 GHz, 2 MW gyrotron is numerically verified by considering the nominal operating conditions and the perfectly aligned GlidCop Al-15 insert. The main focus of this work is the validation of the insert cooling system when the constant temperature of 27 °C is

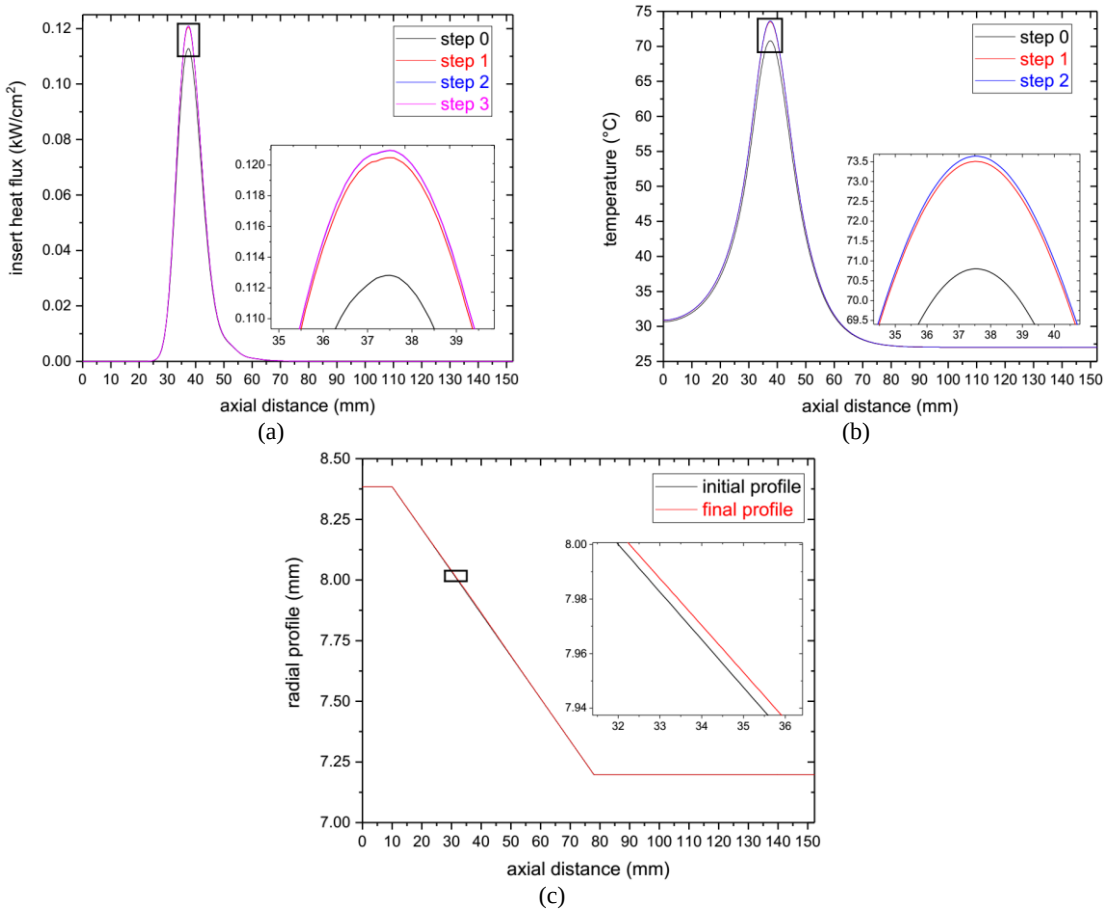

Figure 7: (a) Heat flux and (b) temperature profile at the outer wall of the coaxial insert, supposed perfectly aligned and under the nominal operating conditions. (c) The original and final profiles of the outer wall of the coaxial insert.

assumed for the cavity. The simulation approach discussed in section 2 is applied and the results are summarized in Table I. The initial heat flux (at room temperature (27 °C)) on the non-deformed insert is calculated from the first EM simulation. However, for the successive EM simulations for the next iterations, the temperature field from the TH simulation and the deformed insert geometry from TM simulation are used.

The performance of the transient and stationary approach for the TH simulations have been compared in [35] for the cavity cooling system of a 170 GHz 1 MW hollow-cavity gyrotron and similar results have been achieved with both approaches. Therefore, a simple stationary approach is selected for this study, in which the field is stabilized before the next stage.

After iterative simulations, the insert heat flux profiles, as well as the temperature profiles and the final deformed geometry are presented in Figure 7. The final temperature profile of water is shown in Figure 8. The convergence condition of this iterative simulations is satisfied when the new heat flux calculated by EURIDICE is not more than 0.2 % different from that used in the previous step. The results indicate convergence after three iterative steps, numbered from 0 to 2, each one starting with the electromagnetic simulation, the heat flux calculated at the beginning of step 3 having fulfilled the above-said criterion. The maximum insert loading is 0.121 kW/cm^2 (after 2 steps) and the maximum temperature of the water is 65°C, which is far below the boiling point. The results of TM simulations are plotted in Figure 9. The fields of directional and total deformations look always as expected and the maximal equivalent stress remains largely lower than the limit of elasticity (see Table I), which is 338 MPa according to the producer of GlidCop [36].

Overall, the maximum temperature of the water is below the boiling temperature and the deformations of the insert geometry are small, which does not influence the performance of the gyrotron, significantly. The results, therefore, confirm that a gyrotron equipped with a coaxial insert made of GlidCop Al-15, having the same geometry as the existing insert can operate trouble-free under the foreseen conditions.

Table I: Important results of the three simulations in the case of the perfectly aligned insert under nominal operating conditions. (The deformations are always given relative to the original geometric configuration.)

simulation		step 0	step 1	step 2	step 3
EM	maximum heat flux at wall (kW/cm^2)	0.113	0.120	0.121	0.121
TH	maximum temperature in GlidCop (°C)	70.8	73.5	73.7	
	maximum temperature in water (°C)	62.8	65.0	65.1	
	maximum heat flux at the GlidCop-water interface (kW/cm^2)	0.087	0.093	0.093	
TM	maximum equivalent stress (MPa)	44	47	47	
	maximum radial deformation (μm)	5.3	5.6	5.6	
	maximum axial deformation (μm)	17.3	18.3	18.4	

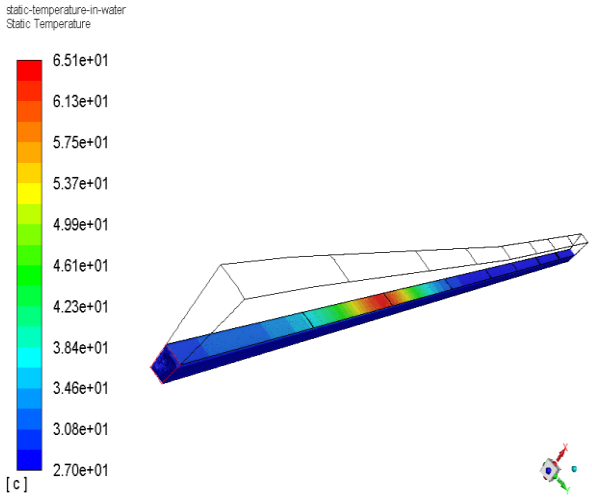

Figure 8: The final temperature profile of the water using the SST k-ω turbulence model. The maximum water temperature reaches 65°C.

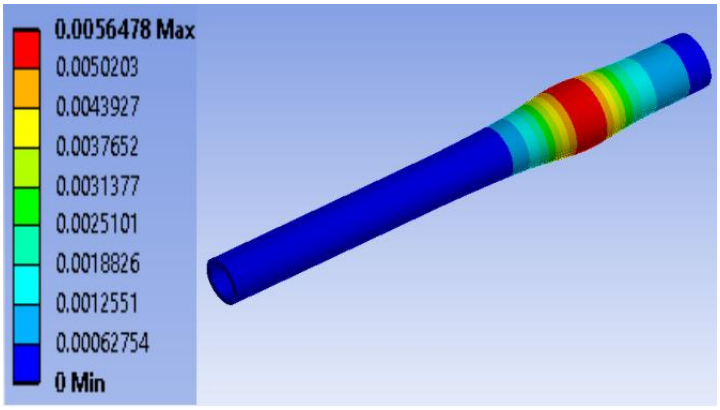

(a)

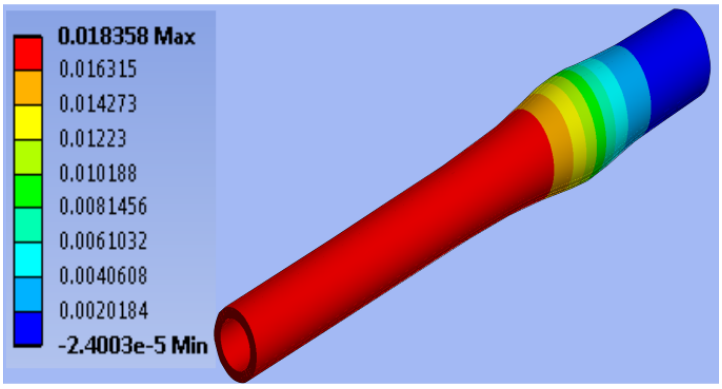

(b)

Figure 9: Insert deformation profile in (a) radial and (b) in axial direction (not to scale). The maximum deformation in the radial and axial direction are only 5.6 µm and 18.4 µm, respectively.

3.1 Parametric study to investigate operational limits

After successfully validating the existing insert cooling system for a CW gyrotron operation, the operational limits of the maximum wall-loading are determined. Two ways were possible to increase the initial heat flux: either increasing the electron beam current and consequently the generated microwave power without changing the geometry of the insert or increasing the radius of the insert without changing the electron beam current, which moves the outer surface of the insert closer to the mode maxima.

Case I: Increasing the initial beam current with unchanged insert geometry:
We started with studying a case in which the electron beam current had been increased to get a maximum initial heat flux of 0.212 kW/cm^2, i.e. almost twice the initial maximum (0.113 kW/cm^2) obtained in the standard case (after the first electromagnetic simulation). The results of this analysis are summarized in Table II. Same as in the previous case, convergence is reached after three iterations, without any water boiling or significant deformation. The calculated maximum water temperature has slightly exceeded 100°C. From this study, we can conclude that the foreseen perfectly aligned insert can stand operating conditions as high as twice the nominal insert loading.

Case II: Increasing the radius of the coaxial insert with unchanged initial current:
In this study, the overall insert outer radius is increased by (a) 0.175 mm and (b) 0.275 mm. With the increase in the overall outer insert radius, the radius of the inner water channel and its wall is slightly increased to maintain the same water velocity. The EM simulations are performed with the nominal gyrotron operating parameters with the updated insert radii. In the first scenario (insert radius increased by 0.175 mm), convergence is achieved in three iterative steps and the maximum water temperature reaches 105.9°C in the final stage with the maximum insert loading of 0.255 kW/cm^2. While in the second scenario (insert radius increased by 0.275 mm), convergence is achieved in five iterative steps and the maximum water temperature is increased to 148.4°C with the maximum heat flux of 0.39 kW/cm^2. In the final state, the equivalent stress remains by far lower than the limit of elasticity. As the margin between the calculated maximum temperature in water and the boiling temperature under the calculated pressure conditions, i.e. 160°C at least, is only 7.25 %, case II with larger insert radius is not selected for further study. In both cases, the deformations are not such large that they result in severe losses of gyrotron performance. The maximum equivalent stress in the GlidCop remains far under the limit of elasticity of the material. In this case, the water boiling seems to be the limiting phenomenon.

Table II: Summery of the operational limit analysis for the insert cooling system

		Case I:	Case II (a): (Δr = 0.175 mm)	Case II (b): (Δr = 0.275 mm)
maximum initial heat flux at wall	kW/cm^2	0.212	0.223	0.318
maximum final heat flux at wall	kW/cm^2	0.243	0.255	0.389
	against the initial conditions (0.121 kW/cm^2)	200.6%	211.0%	321.9%
maximum final temperature in water	°C	101.1	105.9	148.4
maximum final equivalent stress	MPa	92	96	145
	against the limit of elasticity (338 MPa)	27.2%	28.4%	42.9%

4. Study of a misaligned coaxial insert

Up to now, the coaxial insert was supposed to be perfectly aligned in the centre of the cavity. However, a perfect alignment cannot be guaranteed at each time-point during gyrotron operation. A misalignment of the insert' results in a loss of the axil symmetry of the heat flux, which leads to a non-uniform temperature field and to insert-deformation. Therefore, it is important to determine the value of maximum tolerable insert misalignment for stable gyrotron operation. A simple schematic of the axial misalignment of the insert in a coaxial cavity gyrotron is shown in Figure 10. An influence of axial misalignment on the RF behavior of a 240 GHz coaxial cavity gyrotron has been systematically studied in [18]. The results of these studies suggest maximum allowable insert misalignment (D) of 150 μm for the operating frequency

of 240 GHz (D/λ = 0.119), which can be translated to 200 μm for 170 GHz gyrotron (D/λ = 0.113). Here, λ is the free-space wavelength of the generated RF wave. In this work, we are investigating the influence of insert misalignment on the efficiency of the existing cooling system and on the insert geometry.

Due to the axial misalignment of the insert, the direct calculation of the heat flux using the EURIDICE code-package is no longer possible. However, an indirect approach is used to calculate the heat flux. The insert is divided into a certain number of angular sectors. For each sector, the middle position on the outer wall is calculated, then the EURIDICE code-package is used to calculate the heat flux on the surface of a perfectly aligned insert whose radius would be equal to the distance between the cavity axis and the position. As the heat flux is no longer axisymmetric but only symmetric with respect to the plane in which the insert has been displaced, a 10° angular sector is no longer enough for the calculations in Fluent. The angle must be increased to 180° and the rotational periodicity condition to be replaced with a planar symmetry condition. Therefore, the study is continued with the half geometry, which for the calculation and application of the heat flux at the wall was divided into eighteen 10° sectors.

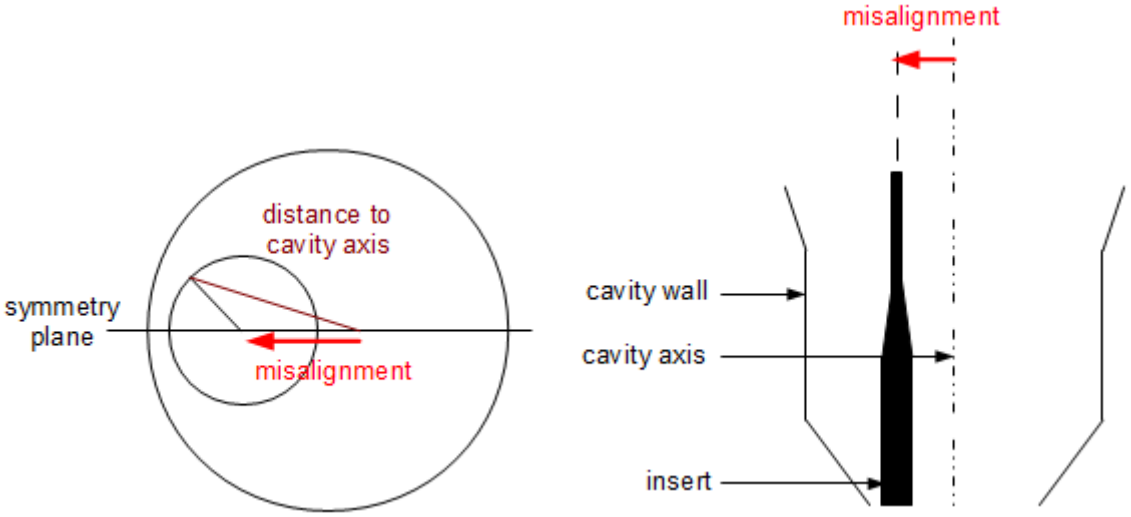

Figure 10: Simple schematic of the axial misalignment of insert in a coaxial cavity gyrotron.

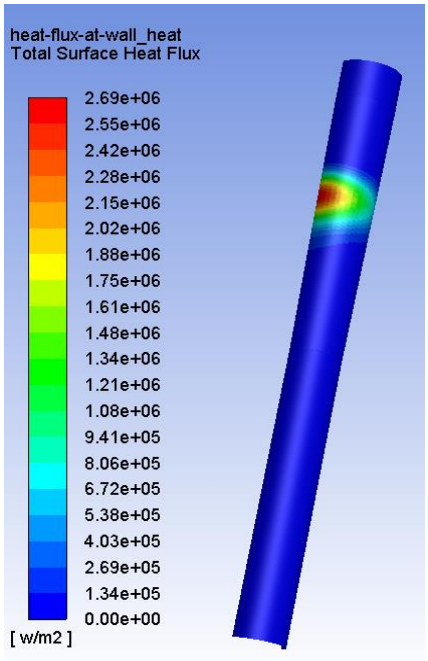

Figure 11: Final heat flux profile on the surface of the insert initially misaligned by 200 μm with respect to the cavity axis.

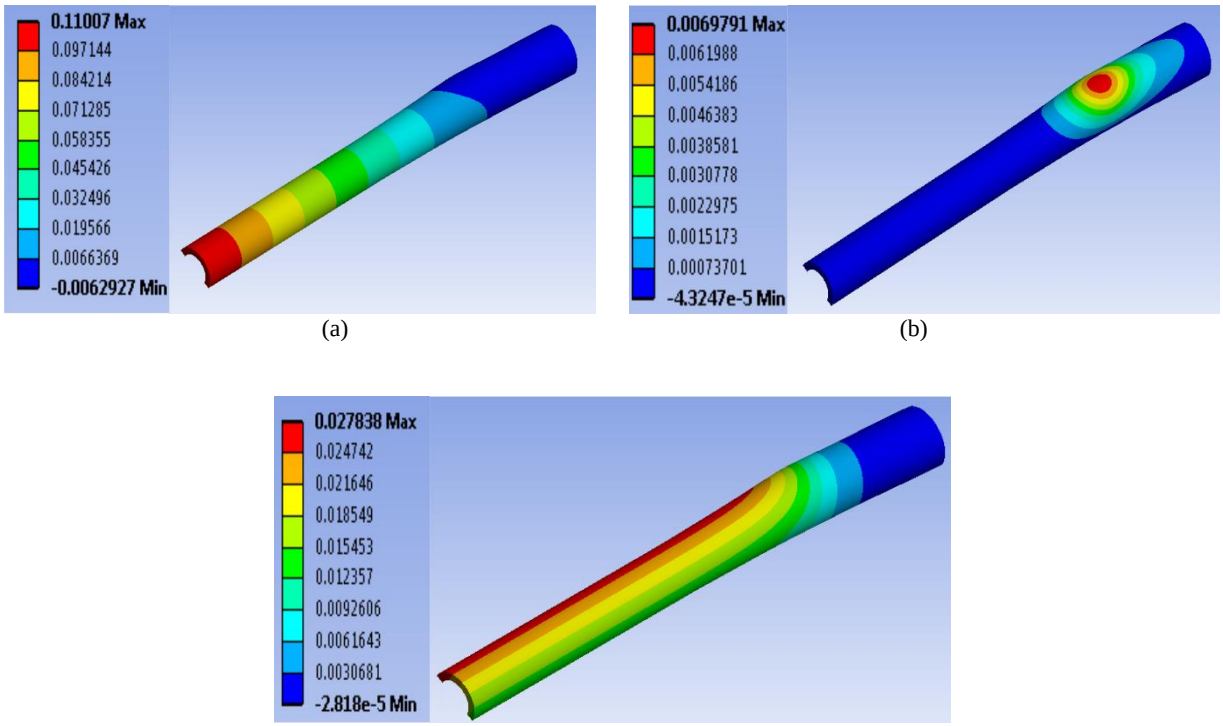

Figure 12: For the insert misalignment of 200 µm, insert deformation in (a) X- direction (b) Y-direction and (c) Z-direction (not to scale). The insert is misaligned in the negative X-direction.

Considering the EM limit of axial misalignment, an insert misalignment of 200 µm is selected for this analysis. The final heat flux on the surface of the insert is presented in Figure 11 and the results of the directional deformations are plotted in Figure 12. The simulation results are summarized in Table III. Indeed, the water temperature remains far from its boiling temperature, and the equivalent stress in GlidCop does not reach even 15 % of the limit of elasticity of the material. Due to transversal deformations, they mostly consist in a bending in the opposite direction of the maximum heat flux, i.e. the direction opposite to the initial shift. This displacement is maximum at the end of the cavity. As the part of the insert located in the launcher is not ohmically-loaded, to determine the final deformation, this result can be extrapolated using trigonometry. Taking into account the length of this part (151 mm), the bending to the axis reaches 220 µm at its maximum. Thus, an initial misalignment of 200 µm still does not result in unacceptable thermomechanical conditions and the combination of this misalignment and the compensating bending does not lead to critical operating conditions.

Table III: Results of the three simulations in the case where the coaxial insert is initially misaligned by 200 µm with respect to the cavity axis and put under nominal operating conditions.

simulation		step 0	step 1	step 2	step 3
EM	maximum heat flux at wall (kW/cm^2)	0.243	0.267	0.269	0.269
TH	maximum temperature in GlidCop (°C)	99.6	105.8	106.4	
	maximum temperature in water (°C)	83.8	88.5	89.0	
TM	maximum equivalent stress (MPa)	51	54	55	
	maximum deformation in the X-direction (µm)	98.5	109.2	110.1	
	maximum deformation in the Y-direction (µm)	6.4	6.9	7.0	
	maximum axial deformation (µm)	25.7	27.7	27.8	

5. Conclusions

In this work, the performance of the insert cooling system of a coaxial gyrotron cavity is systematically studied for continuous wave gyrotron operation. Additionally, the operational limits of the insert cooling system are determined with respect to the maximum allowable heat-flux and axial misalignment. A multi-physics simulation model has been developed with the SST k-ω turbulence model and relevant mesh parameters. Considering the nominal gyrotron operating parameters, the results suggest stable operation of the GlidCop insert with the existing design. The maximum insert heat flux is 0.12 kW/cm^2 for a perfectly aligned insert under the nominal operating conditions. However, the insert can withstand heat-fluxes up to 0.39 kW/cm^2. For all the discussed cases, the maximum equivalent stress is lower than 43 % of the limit of elasticity of GlidCop and the deformations of the material do not result in significant degradation of gyrotron performances. However, the water boiling point is the only limiting phenomenon for each case. A misalignment of the foreseen insert, provided that, it does not exceed 200 µm (which is the EM limit for the excitation of the desired operating mode), is far from resulting in water boiling or plastic deformations and the gyrotron is still capable of proper operation. The experimental validation of the insert cooling system is ongoing at KIT-IHM. Joint multi-physics simulations of both the insert and cavity cooling systems are planned.

6. Acknowledgement

This work has been carried out within the framework of the EUROfusion Consortium and has received funding from the Euratom research and training programme 2014-2018 under grant agreement No 633053. The views and opinions expressed herein do not necessarily reflect those of the European Commission. Parts of the simulations presented in this work have been carried out the Marconi-Fusion super-computer facility.

7. Appendix: Selection of mesh parameters for thermal-hydraulic simulations

Theory predicts – and the simulation results later confirmed – that the largest temperature gradients are to be found in water, at or in the vicinity of the interface with the solid. The mesh refinement effort must be concentrated in this region. Therefore, an inflation function is applied at the water inlet face from its boundary with the solid (refer Figure 13). The user indicates to Fluent the first mesh layer thickness and the maximum number of layers in the inflation zone. The thickness of each one is calculated (except for the first one) by multiplying that of the lower layer by a user-specified growth rate. The transition ratio, i.e. the ratio of the thicknesses of the first layer outside the inflation zone and the last layer in this zone, is also specified by the user.

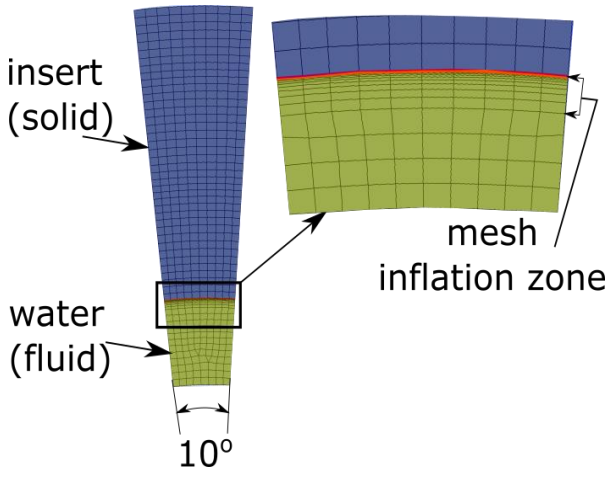

Figure 13: Selected mesh inflation zone at the solid-fluid interface.

To ensure that these criteria are respected in the whole fluid domain a mesh sweeping method is selected. For the selected turbulence model, the inflation layer parameters are fixed by considering the dimensionless distance from wall, y^+, which is defined by [37],

$$y^+ = \frac{y u_\tau}{\nu}. \tag{2}$$

Here, y provided that the distance from the wall to the upper limit of the current element, ν is the kinematic viscosity of the fluid and u_τ is defined by,

$$u_\tau = \sqrt{\frac{\tau_w}{\rho}}. \tag{3}$$

Here, τ_w is the wall shear stress vertically from the element and ρ the fluid density. For the SST k-ω model and the recent versions of Fluent, it is recommended to have y^+ not higher than 1 for the first layer and at least 10 mesh layers in the inflation layer, whose y+ value should be less than 200 for this kind of problems [38]. After systematic investigation of the inflation layer parameters, the first layer thickness of 1.5×10^{-3} mm and 10 inflation layers are selected with a growth rate of 1.4 to get the y^+ value of the first layer less than 1. With the selected growth rate, the value of y^+ of the 10th layer is also less than 200. The value of y^+ for the first layer is checked and maintained less than 1 for each iteration. After the first step, the minimum orthogonal quality of the selected mesh is 0.93 with its average value of 0.99.

8. References

[1] Thumm M. 2016 *State-of-the-art of high power gyro-devices and free electron masers, update 2017* Sci. Rep. KIT-SR 7750.

[2] Kartikeyan M. V. *et al*, 2004, *Gyrotrons – High Power Microwave and Millimeter Wave Technology*, Springer–Verlag, Berlin–Heidelberg.

[3] Thumm M. 2014 *IEEE Trans. Plasma Sci.* **42** 590-99.

[4] Erckmann V. *et al*, 2014 *AIP Conf. Proc*. **1580**, 542.

[5] Litvak A. *et al* 2011 *Plasma Phys. Control. Fusion* **53** 124002.

[6] Denisov G. G. *et al* 2008 *Nucl. Fusion* **48** 054007.

[7] Kasugai A. *et al* 2008 *Nucl. Fusion* **48**, 054009.

[8] Kalaria P. *et al* 2014 *IEEE Trans. Plasma Sci*. **42** 1522-28.

[9] Poli E. *et al* 2013 *Nucl. Fusion* **53** 013011.

[10] Granucci G. *et al* 2017 *Nucl. Fusion* **57** 116009.

[11] Jelonnek J. *et al* 2017 *Fusion Engineering and Design* **123** 241-246.

[12] Tran M. Q. *et al* 2016 *26th IAEA Fusion Engineering Conference*, Kyoto, Japan.

[13] Franck J. *et al* 2014 *IEEE International Vacuum Electronics Conference*, Monterey, CA.

[14] Thumm M. *et al* 2015 *International Journal of Terahertz Science and Technology* **8** 85-128.

[15] Kalaria P. *et al* 2016 *Physics of Plasmas* **23** 092503.

[16] Schmid M. *et al* 2015 *Fusion Engineering and Design* **96-97** 589-92.

[17] Kalaria P. *et al* 2017 *Frequenz* **71** 161-171.

[18] Franck J. 2017 *Systematic Study of Key Components for a Coaxial-Cavity Gyrotron for DEMO*, KIT Scientific Publishing, Karlsruhe.

[19] Kalaria P. 2017 *Feasibility and Operational Limits for a 236 GHz Hollow-Cavity Gyrotron for DEMO*, KIT Scientific Publishing, Karlsruhe.

[20] Pagonakis I. Gr. *et al 2015 Fusion Engineering and Design* **96-97** 149-154.

[21] Rzesnicki T. *et al* 2017 *Fusion Engineering and Design* **123** 490-494.

[22] Ioannidis Z. *et al* 2017 *IEEE Trans. on electron devices* **64** 3885-92.

[23] Rzesnicki T. *et al* 2010 *IEEE Trans. Plasma Sci*. **38** 1541-49.

[24] Ruess S. *et al* 2017 *EPJ Web of Conferences* **149** 04015.

[25] Denisov G. 2017 *EPJ Web of Conferences* **149** 01001.

[26] Sakamoto K. *et at* 2013 *IEEE International Vacuum Electronics Conference,* Paris, France.
[27] Oda Y. *et at* 2017 *EPJ Web of Conferences* **149** 01002.
[28] Bertinetti A. *et al* 2017 *Fusion Engineering and Design* **123** 313-16.
[29] Savoldi L. *et al* 2016 *IEEE Trans. on Plasma Science* **64** 3885-92.
[30] Savoldi L. *et al* 2015 *IEEE Symposium on Fusion Engineering,* Austin, TX, USA.
[31] Avramides K. A. *et al* 2017 *IEEE International Vacuum Electronics Conference,* London, UK.
[32] Avramides K. A. *et al* 2012 *17th Joint Workshop on Electron Cyclotron Emission and Electron Cyclotron Resonance Heating,* Deurne, The Netherlands.
[33] Jackson J. D. 1975 *Classical Electrodynamics,* Second edition, Wiley
[34] Shojiro O. 1993 *Mechanical properties of metallic composites,* CRC Press.
[35] Avramidis K. A. *et al* 2018 *IEEE Transactions On Electron Devices* **99** 1-8.
[36] Höganäs (North American), 2015, GLIDCOP® Mechanical Properties as Drawn Rod+ & Rolled Strip Tempers, Technical Data Sheet.
[37] ANSYS Fluent Theory Guide, Release 18.0, January 2017.
[38] Alessandro Vaccaro, KIT, Institute for Applied Materials (IAM), private communication.